POLISH POLAR RESEARCH
vol. 37, no. 3, pp. 379–402, 2016 doi: 10.1515/popore-2016-0020

Climate projections in the Hornsund area, Southern Spitsbergen

Marzena OSUCH and Tomasz WAWRZYNIAK

Institute of Geophysics, Polish Academy of Sciences, ul. Księcia Janusza 64, 01-452 Warszawa, Poland
<marz@igf.edu.pl> <tomasz@igf.edu.pl>

Abstract: The aim of this study was to provide an estimation of climate variability in the Hornsund area in Southern Spitsbergen in the period 1976–2100. The climatic variables were obtained from the Polar-CORDEX initiative in the form of time series of daily air temperature and precipitation derived from four global circulation models (GCMs) following representative concentration pathways (RCP) RCP 4.5 and RCP 8.5 emission scenarios. In the first stage of the analysis, simulations for the reference period from 1979 to 2005 were compared with observations at the Polish Polar Station *Hornsund* from the same period of time. In the second step, climatic projections were derived and monthly and annual means/sums were analysed as climatic indices. Following the standard methods of trend analysis, the changes of these indices over three time periods – the reference period 1976–2005, the near-future period 2021–2050, and far-future period 2071–2100 – were examined. The projections of air temperature were consistent. All analysed climate models simulated an increase of air temperature with time. Analyses of changes at a monthly scale indicated that the largest increases were estimated for winter months (more than 11°C for the far future using the RCP 8.5 scenario). The analyses of monthly and annual sums of precipitation also indicated increasing tendencies for changes with time, with the differences between mean monthly sums of precipitation for the near future and the reference period similar for each months. In the case of changes between far future and reference periods, the highest increases were projected for the winter months.

Key words: Arctic, Svalbard, climate change, climate projections.

Introduction

It is widely acknowledged that the climate of the Arctic, defined as the region north of 60°N, has undergone a warming during the past 100 years. This warming is twice as intense as the global warming and is known as Arctic amplification (Miller *et al*. 2010; Cohen *et al*. 2014). Model simulations of the future climate show that Arctic amplification is predicted to continue and

accelerate in the upcoming decades (Serreze *et al*. 2009; Koenigk *et al*. 2015). The linear trend in air temperature in the European Arctic, particularly in the Svalbard Archipelago, indicates an increase in mean annual temperature of 2.6°C during the last 100 years (Przybylak 2003; Stocker *et al*. 2013; Nordli *et al*. 2014; Koenigk *et al*. 2015), about three times higher than the estimated global warming for this period of time (0.8°C). The cause of the difference in warming rates is very complex and still not well understood. Climate variability in the Arctic operates on wide range of spatial and temporal scales (Przybylak 2003; Goosse 2015). Although all seasons have experienced an increase in temperature over the past several decades, the warming trend has been most pronounced in the winter season (Bintanja and van der Linden 2013). Lack of solar radiation, which during polar day is a dominant factor affecting temperature increase, makes the late autumn, winter and early spring the most unstable seasons in terms of thermal conditions (Bednorz and Kolendowicz 2013). Strong decadal, inter-annual as well as seasonal and synoptic scale variations are also present.

Variations of air temperature and precipitation have pronounced effects on many aspects of both the abiotic and biotic components of Arctic ecosystems, which are highly vulnerable to changes. It is well known that regional climate change directly affects the local climate on a temporal scale, thus analyses of climate variability and trends on local scales are key in understanding and predicting the sensitivity of high-latitude ecosystems (*e.g*. Larsen *et al*. 2014; Goosse 2015; Vormoor *et al*. 2015; Wawrzyniak *et al*. 2016).

The best modern tools that allow for physically based descriptions of the future development of climatic conditions are global circulation models (GCMs), which are built based on physical laws describing major physical processes related to the atmosphere, oceans, sea ice and land surface. The spatial resolution of GCMs of around 1000 x 1000 km, is too low to accurately resolve important processes at regional and local scales (Goosse 2015). The climate simulations at higher resolutions are achieved with help of regional climate models (RCMs) nested in the GCMs. The coupling of GCMs with RCMs allows for a higher spatial resolution and improves simulation results of many processes (Koenigk *et al*. 2015). The climate models are stimulated by external forcings that influence major climate variations. These forcings include greenhouse gases, aerosols, various pollutants in the atmosphere and others (Goosse 2015). The future evaluations of climatic conditions are conducted with help of emission scenarios that are estimates of future changes in these forcings. There are many types of scenarios but the results of climate models generally are based on the older scenarios described in the Special Report on Emission Scenarios (SRES) (Nakicenovic *et al*. 2000) and used in the fourth assessment report of the Intergovernmental Panel on Climate Change (IPCC AR4; Solomon *et al*. 2007) or newer scenarios in the form of four representative concentration pathways (RCP) presented in Moss *et al*. (2010) and applied in the fifth IPCC assessment report (IPCC AR5; Stocker *et al*. 2013).

The analysis of climate development in the Arctic has been performed by several authors (*e.g.* Kattsov and Walsh 2000; Przybylak 2003; Rinke *et al.* 2006; Rinke and Dethloff 2008; Førland *et al.* 2011; Matthes *et al.* 2011; Overland *et al.* 2011; Rinke *et al.* 2011; Glisan *et al.* 2013; Glisan and Gutowski 2014; Overland *et al.* 2014; Koenigk *et al.* 2015), but mostly at a regional scale. The analyses in the framework of the Arctic Climate Impact Assessment, ACIA (ACIA 2005), indicate an increase of Arctic mean annual temperature of 7°C and 5°C for the A2 and B2 emission scenarios and annual precipitation totals by 12% in 2071–2100 with respect to 1981–2000.

Following the results presented in the IPCC Fourth Assessment Report (Solomon *et al.* 2007), the mean warming in the end of the 21st century ranges from 4.3°C to 11.4°C in winter and from 1.2°C to 5.3°C in summer for the A1B emission scenario. The changes (18%) in the mean Arctic precipitation were estimated as median from the ensemble of climate models.

The IPCC Fifth Assessment Report (Stocker *et al.* 2013) states that the Arctic region will continue to warm more rapidly than the global mean by the end of the century. The projected changes in annual mean temperature averaged over the Arctic (67.5°N to 90°N) are 4.2°C and 8.3°C for scenarios RCP 4.5 and RCP 8.5 respectively. The changes in precipitation are predicted to be almost linearly related to near surface air temperature (Stocker *et al.* 2013).

The projected changes in air temperature and precipitation are unevenly distributed over the Arctic. Koenigk *et al.* (2015) analysed an ensemble of four GCMs downscaled over the Arctic with one RCM. Their results indicate the strongest change in autumn and winter with significant spatial differences. The highest warming during the autumn was achieved for areas between 82°N and 90°N while during winter, the most warming was predicted in the area between 78°N and 85°N over the Barents Sea. Due to such spatial variation in the projections, there is a need for detailed scenarios for more specific locations in the Arctic, *e.g.* Southern Spitsbergen and the Hornsund area.

The spatial distribution of air temperatures in Svalbard from one year of observations at 30 sites was described by Przybylak *et al.* (2014). The analysis of air temperature and precipitation development at Svalbard was carried out by Førland *et al.* (2011). In that study, the climate variables were simulated by the regional climatic model HIRHAM2/NorACIA nested in six global climatic models. The projections used (A2, B2, and A1B) were based on the earlier SRES emission scenarios (Nakicenovic *et al.* 2000). The simulations were validated using observations from two measurement sites: Longyearbyen Airport in Spitsbergen, Svalbard, and Bjørnøya. The estimated median change from the ensemble of mean annual air temperatures for Longyearbyen was 6.6°C between 2071–2100 and 1961–1990 periods. The largest changes, exceeding 10°C, were obtained for winter months. The results for Bjørnøya indicated less intense warming (5.5°C) than for Longyearbyen and also less seasonal variation of projected changes.

This study represents the first attempt to project climate conditions in Southern Spitsbergen using climate scenarios from the Polar-CORDEX initiative based on RCP emission scenarios. We focus on the comparison of observational and modelled data from the Hornsund area and provide results of climate projections until the end of the 21st century. The simulated climatic variables are obtained from the Polar-CORDEX initiative in the form of time series of daily air temperature and precipitation derived from four most current GCMs following two most recent emission scenarios RCP 4.5 and RCP 8.5. In this work, we validate the climate simulations on the observations at Polish Polar Station *Hornsund* in the period 1979–2005 and analyse the simulated air temperature and precipitation from the period 1976–2100. Within that time period, the changes of air temperature and precipitation over three time periods (1976–2005, 2021–2050 and 2071–2100) are examined.

Study area

The study area is located in Hornsund on Southern Spitsbergen (Fig. 1), the largest island of the Svalbard archipelago in the Euro-Atlantic sector of the Arctic. Spitsbergen is surrounded by cold waters of the Arctic Ocean in the north, the Barents Sea in the southeast, and the Greenland Sea in the southwest, which is warmed by the West Spitsbergen Current, a branch of the North Atlantic Current. Polish Polar Station *Hornsund* is located 300 m from the northern shore of Hornsundfjord on the uplifted marine terrace with abundant tundra vegetation, 10 m above sea-level, at the geographical coordinates 77° 00' N 15° 33' E. At this latitude, the polar night starts in the end of October and lasts until the middle of February. Without solar radiation, atmospheric and oceanic circulations have a major impact on heat transfer and thereby climatic conditions. The meteorological station has operated constantly in the synoptic recording regime with standard and automatic instruments as well as visual observations since July 1978, and has provided one of the longest observational series available for Svalbard. For the validation, data from the period 1979–2005 were used, when the mean annual air temperature was -4.5°C. The mean monthly air temperatures in Hornsund for this period show a long and cold period of polar winter (December–April) with the mean temperature around -10°C (Fig. 3). The summers in the study area are short, and the mean monthly air temperatures for summer period (June–September) reach slightly above 0°C, but do not exceed 5°C.

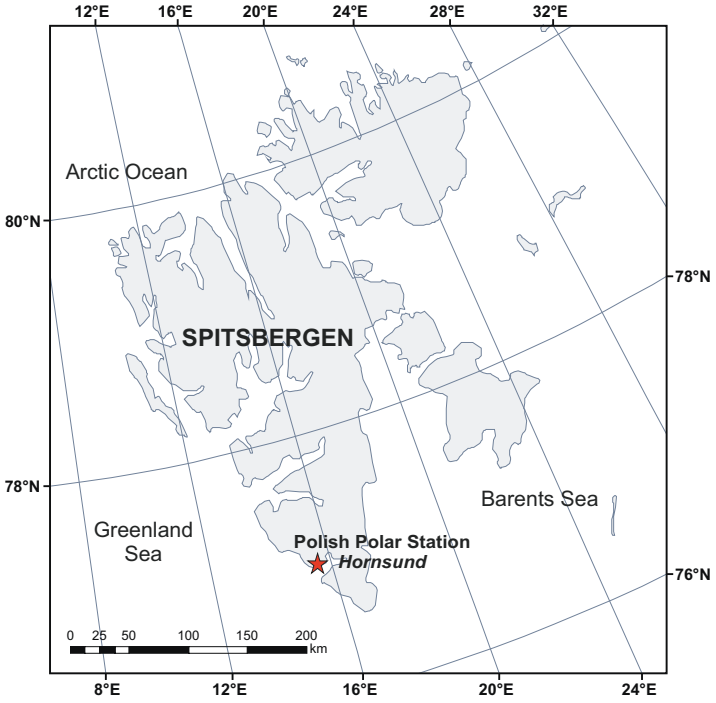

Fig. 1. The study area.

Methods

Climate data. — The analyses were carried out using climate model simulations available from the Coordinated Regional Downscaling Experiment initiative (CORDEX), which provides an improved generation of climate change projections as an input to impact and adaptation studies (Giorgi *et al*. 2009). In the framework of CORDEX, several areas of interest have been selected and analysed. One of areas of interest has been Polar-CORDEX, which provides climate projections in the Arctic and Antarctic domains. The results for the Arctic domain consist of an ensemble of climate model simulations for historical and RCP emission scenarios. Historical simulations are available for the period 1950–2005 while the scenario for the 2006–2100 period is available with daily, monthly and seasonal temporal resolutions. A few modelling centres participate in the Polar-CORDEX initiative. Due to data availability for historical and future periods, the outcomes from one regional climate model (Rossby Centre Atmospheric Model, RCA4) nested in four global climate models (CCCma-CanESM2, NCC-NorESM1-M, ICHEC-EC-EARTH, MPI-M-MPI-ESM-LR) were analysed in this study. The RCA4 model is the newest version of the Rossby Centre

Atmospheric Model based on the numerical weather prediction model (High Resolution Limited Area Model, HIRLAM). A detailed description of the model is presented in Koenigk *et al*. (2015).

In the four tested cases, the spatial resolution of regional model was set to 0.44° on a rotated latitude-longitude grid in rotated coordinates with a quasi-uniform resolution of approximately 50 x 50 km. The results of simulations for the Arctic domain are available in the form of matrix with 116 x 133 grid cells. These cells have defined coordinates which allow selecting an appropriate grid cell closest to the area of the interest. In Fig. 2, a map of the Arctic domain from the applied models is shown together with the grid cell, which was selected to represent local climatic conditions in the vicinity of Polish Polar Station *Hornsund*. The selected grid cell covers most part of Southern Spitsbergen, including surroundings of Hornsundfjord and Sørkappland. This area is highly glaciated and mountainous; thus, local climatic conditions are strongly differentiated. Because of large climate gradients and the harsh weather conditions, even small differences between locations of measuring sites may cause substantial changes in observed conditions. Climate simulations provide areal means of those conditions over 50 x 50 km, although there are pronounced spatial differences of topoclimatic conditions which are usually described over distances from 100 m to 1–10 km. Gridded data sets have a smoothing effect, which is much higher for precipitation than for temperature (Wibig *et al*. 2014).

The climate scenarios available at Polar-CORDEX were calculated for emission scenario defined in the Fifth Assessment Report of the IPCC and explained in detail in Moss *et al*. (2010). These greenhouse gases and atmospheric pollutant emission scenarios (Representative Concentration Pathways, RCP) do not specify socioeconomic scenarios, but assume pathways of different radiative forcings at the end of the 21st century. In the Polar-CORDEX, as well as in this paper, two emission scenarios were analysed: RCP 4.5 and RCP 8.5. Increases in the radiative forcing of 4.5 and 8.5 W/m^2 in the end of the century compared to pre-industrial conditions are assumed by the RCP 4.5 and 8.5 scenarios, respectively. RCP 8.5 is the most extreme scenario and displays a continuous rise in radiative forcing with emissions three times greater than in year 2000. RCP 4.5 is characterised by a steadier rise and emissions slightly higher than in 2000 (Goosse 2015). The Polar-CORDEX repository provides a number of climatic variables, including daily mean air temperature at 2 m above the ground and daily sum of precipitation; both are analysed in this paper.

Trend analysis. — The tendency of changes in mean annual and monthly air temperature and precipitation were estimated using the trend analysis method by Mann-Kendall (Mann 1945; Kendall 1975). There are many techniques that can be used to estimate trends in the time series, such as linear regression, Spearman's rho test, Mann-Kendall test, seasonal Kendall test, and application

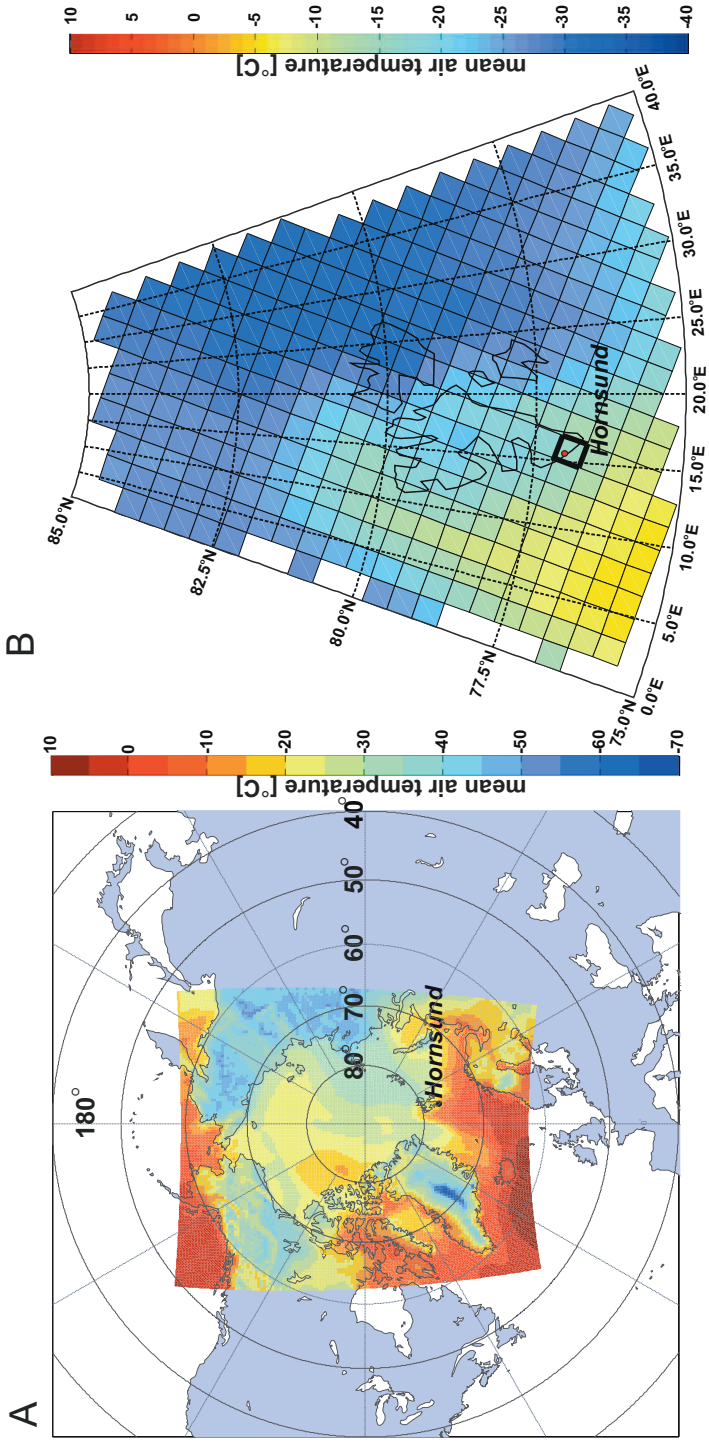

Fig. 2. **A.** The Arctic domain applied in the four tested models. **B.** The grid cell that represents climatic conditions in the vicinity of Polish Polar Station *Hornsund*. The colour bar represents mean air temperature [°C] on January 1, 1976, simulated by CCCma-CanESM2.

of time series models (Kundzewicz and Robson 2004). The choice of method strongly depends on the analysed data, as the methods differ in their assumptions and requirements. In the Mann-Kendall test, there is no assumption related to the distribution of residuals, as is the case for a linear regression.

The Mann-Kendall test for trend analysis is based on a rank correlation test of the observed values and their order in time. In this case the Mann-Kendall test statistics, S is calculated from the following equation:

$$S = \sum_{k=1}^{n-1} \sum_{j=k+1}^{n} \operatorname{sgn}(x_j - x_k) \quad \text{where}$$

$$\operatorname{sgn}(x_j - x_k) = \begin{cases} +1 & if \quad (x_j - x_k) > 0 \\ 0 & if \quad (x_j - x_k) = 0 \\ -1 & if \quad (x_j - x_k) < 0 \end{cases} \tag{1}$$

and where n is the number of observations. For independent and randomly ordered data for large n, the S statistics approximate a normal distribution with mean E(S) = 0 and a variance equal to var(S) = n(n – 1)(2n + 5)/18.

The significance of the trend is tested by comparison of the standardised test statistics, Z, with the standard normal cumulative distribution at selected a significance level. Positive values of Z statistics indicate a positive trend (an increasing trend) while negative Z values indicate the decreasing trend. The trend is statistically significant at 0.05 significance level when the absolute value of Z is greater than 1.96.

The application of the Mann-Kendall test can be affected by the serial correlation of data and also by seasonality effects, as presented by Hamed and Rao (1998). To avoid problems with autocorrelation a modified Mann-Kendall test has been developed. The modification allows the test to be applied to data with serial correlation, as is the case therein.

To account for the effect of the serial correlation, the correction ratio n/n_S^* was introduced during the calculation of a variance of the S statistics.

$$\operatorname{var}^*(S) = \operatorname{var}(S) \frac{n}{n_S^*} \tag{2}$$

$$\frac{n}{n_S^*} = 1 + \frac{2}{n(n-1)(n-2)} \sum_{i=1}^{n-1} (n-i)(n-i-1)(n-i-2)\rho_S(i) \tag{3}$$

where ρ_S is the autocorrelation function of the ranks of observations.

The slope of the trend can be estimated using the Sen's method, wherein the trend is assumed to be linear (Wilcox 2005). Following that method, the slopes between all data pairs are calculated and then the overall slope is estimated using the median of those slopes. The used median values are not strongly affected by outliers.

Results

Validation of climate simulations in 1979–2005 period

Validation of climate simulations in 1979–2005 period. Air temperature. — In the first stage of analysis, simulations for the reference period (1979–2005) were compared with observations over the same period of time. The analyses were carried out for mean monthly air temperature and the standard deviation of mean monthly air temperature over the reference period. Such a validation procedure allows assessment of the quality of the climate model simulations and confirmation of their suitability for projecting future climate conditions. The results for the first indicator (mean monthly air temperature) are presented in Fig. 3. It is visible that the two climate models, namely NCC-NorESM1-M and ICHEC-EC-EARTH, underestimate the observed air temperature at the *Hornsund* station. The highest differences were estimated for winter with errors up to 7.3°C. The results of two other models (CCCma-CanESM2 and MPI-M-MPI-ESM-LR) resemble the observations in winter months and slightly overestimate them in other months.

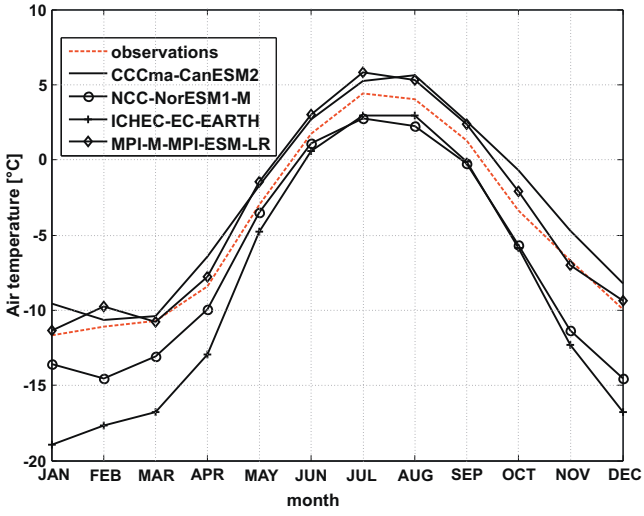

Fig. 3. Comparison of the observed and simulated mean monthly air temperatures over the 1979–2005 period.

Validation of climate simulations in 1979–2005 period. Precipitation. — The performance of climate models in simulating the monthly sum of precipitation was tested. A comparison of mean monthly precipitation totals over 1979–2005 period is presented in Figure 4. In the case of precipitation, all GCM/RCM models overestimated the monthly sum of precipitation observed at the

Hornsund station in all months except in the summer. The differences between observations and simulations are the highest in winter months (almost 60 mm *per* month in January and December for CCma-CanESM2 model).

The comparisons of the simulated and observed air temperature and precipitation indicate that the quality of such simulations depends on the climatic variables. Simulation of precipitation is strongly biased as a result of the simplified description in climate models of the numerous and complex processes that lead to precipitation generation in the atmosphere. This problem is well known and reported by many authors (Sunyer *et al*. 2015; Osuch *et al*. 2016). In the studies of the impact of climate change on processes related to precipitation, the bias correction of the climate simulations relative to observations is used (Madsen *et al*. 2014).

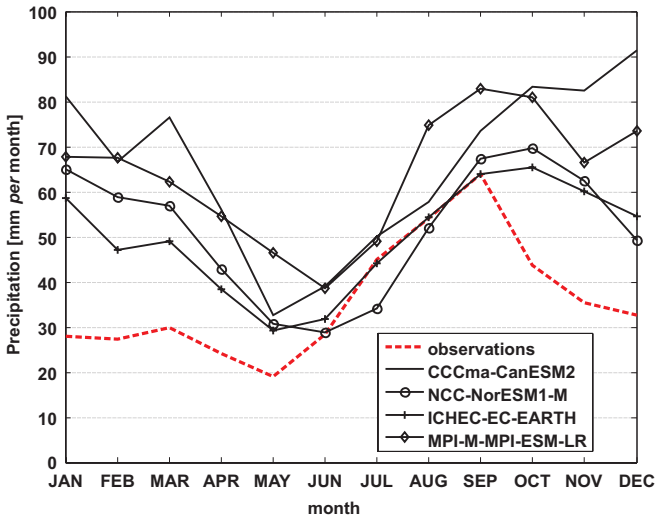

Fig. 4. Comparison of the observed and simulated mean monthly sum of precipitation over the 1979–2005 period.

There is ongoing scientific discussion on the appropriateness of bias correction of data derived from climate model simulations (Christensen *et al*. 2008; Ehret *et al*. 2012; Muerth *et al*. 2013; Teutschbein and Seibert 2013; Osuch *et al*. 2016). An application of a bias correction significantly improves the simulation results in the reference period, but at the same time it might alter a relationship between climate variables and cause a violation of conservation principles. In addition, the consistency between the spatio-temporal fields of climate variables can be altered during bias correction. Another problem is related to an assumption of stationarity of bias correction method parameters derived for a period with available observations and later used for changed conditions in future periods. Application of bias correction in the modelling chain can alter climate change

signals. The most favourable but also the most challenging solution may be achieved by the improvement of climate models so that bias correction is not required, but at the moment such simulations are not available. Therefore, in this study we decided to analyse uncorrected climate model outputs.

Climatic projections 2006–2100. Trend in air temperature. — In the second step of this study, climatic projections were processed and monthly as well as annual means/sums were analysed as climatic indices. Following the standard methods of analysis by trend estimation, the changes of these indices over the three time periods were examined: the reference period (1976–2005), the near-future period clim1 (2021–2050) and far-future period clim2 (2071–2100).

In the case of air temperature, the analyses were carried out for mean annual and monthly air temperature in the period 1976–2100 with the four climate models and two emission scenarios. The estimated mean annual air temperature is presented in Fig. 5. It is clearly visible that there is a positive trend of air temperature over time. All model simulations predict increases of air temperature with different magnitudes of change.

Following the method presented in the preceding section, a trend analysis of mean annual air temperature was conducted. The results of the Mann-Kendall

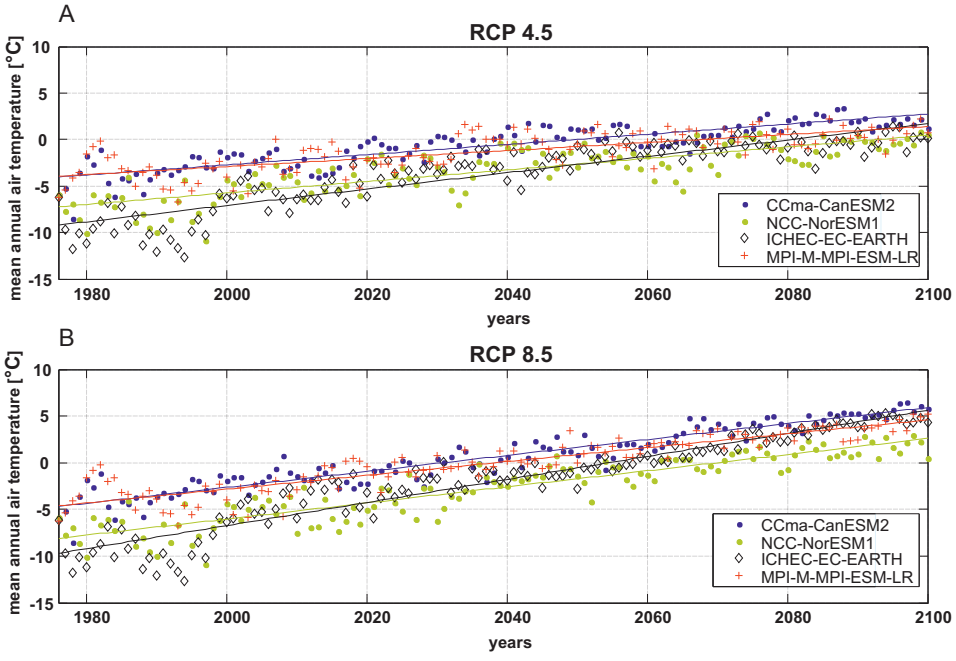

Fig. 5. Comparison of mean annual air temperature simulated by four climate models for two emission scenarios: RCP 4.5 (**A**) and RCP 8.5 (**B**). Both plots together with the estimated linear trends in period 1976–2100.

test indicate that for all tested climate model simulations, the trend is statistically significant at the 0.05 significance level. The slopes of the trends together with the confidence limits were calculated by Sen's method and are presented in Table 1. The estimates of the trend for emission scenario RCP 4.5 vary from 0.0428 [°C *per* year] for MPI-ESM-LR to 0.0594 [°C *per* year] for NorESM1-M. The median from the ensemble in that case is 0.0498 [°C *per* year]. The median slope of the trend for the time series following emission scenario RCP 8.5 is higher [0.0847°C *per* year], indicating more intense changes. The range of slopes estimated for four climate models is about 0.0454°C *per* year. Similar to the results for RCP 4.5, the smallest changes are simulated by MPI-ESM-LR model and highest by NorESM1-M.

Table 1

The slopes of the trend in annual mean air temperature in Southern Spitsbergen [°C *per* year] simulated by four climate models. LCI and UCI denote lower and upper confidence intervals at the 0.05 significance level, respectively.

Model	RCP 4.5			RCP 8.5		
	LCI	Slope	UCI	LCI	Slope	UCI
CanESM2	0.0476	0.0533	0.0596	0.0806	0.0857	0.0904
NorESM1-M	0.0520	0.0594	0.0675	0.0773	0.0837	0.0910
EC-Earth	0.0745	0.0835	0.0919	0.1125	0.1196	0.1264
MPI-ESM-LR	0.0349	0.0428	0.0503	0.0685	0.0742	0.0802
Ensemble median	0.0498	0.0564	0.0636	0.0789	0.0847	0.0907

The results of the trend analyses for mean monthly air temperature are shown in Figure 6. In all cases the trend was statistically significant at the 0.05 significance level. Similar seasonal patterns in the estimated slopes were achieved for both emission scenarios. The smallest slopes were achieved for the summer months (June–September) and the highest for winter months (December–March). More intense changes are projected for emission scenario RCP 8.5 than for RCP 4.5.

Climatic projections 2006–2100. Trend in precipitation. — The results of the trend analysis for annual sum of precipitation (Fig. 7) indicate that the trend is statistically significant for all models. The slopes of the trends and the associated lower and upper confidence limits estimated by Sen's method are shown in Table 2. The median slope of an ensemble of climate models is equal to 2.14 [mm *per* year] for scenario RCP 4.5 and 3.52 [mm *per* year] for scenario RCP 8.5. There are differences in the estimates between the climate models. The largest change in precipitation was simulated with the EC-Earth model for

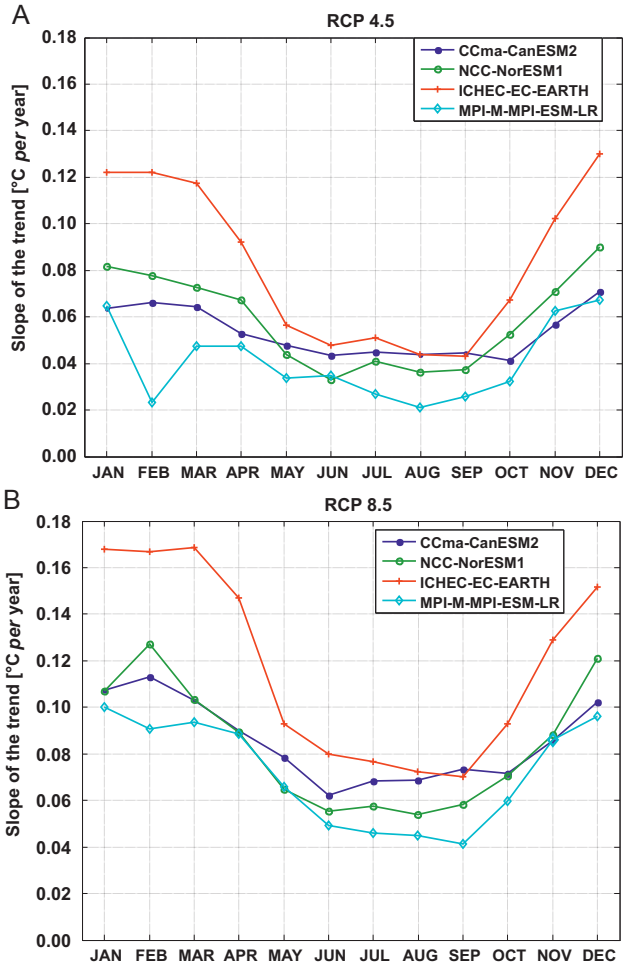

Fig. 6. Slopes of the trend [°C *per* year] estimated for monthly mean air temperature in 1976–2100 for four climate models and two emission scenarios: RCP 4.5 (**A**) and RCP 8.5 (**B**). In all cases the trend was statistically significant at the 0.05 significance level.

RCP 4.5 and CanESM2 for emission scenario RCP 8.5. The smallest increases were simulated by the MPI-ESM-LR model using both emission scenarios.

The estimates of the trend slope for monthly sums of precipitation are shown in Fig. 8. In this case, the statistically significant trend were achieved not for all months and models. The simulations of the MPI-ESM-LR model for scenario RCP 4.5 are characterized by the lack of statistically significant trends for most of months. The trends are statistically significant for the other three climate models for emission scenario RCP 4.5 and for all models for scenario RCP 8.5. Taking into account the magnitude of these changes, the results confirm

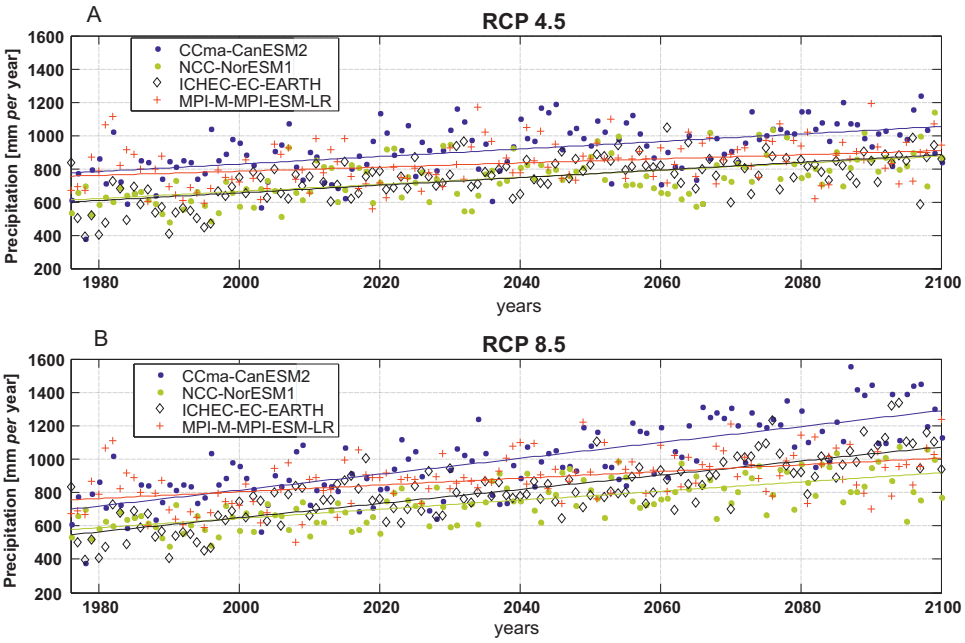

Fig. 7. Projections of annual sums of precipitation [mm *per* year] by four climate models following two emissions scenarios: RCP 4.5 (**A**) and RCP 8.5 (**B**).

findings presented in the section describing changes in precipitation between two future and reference periods. Larger changes were projected for emission scenario RCP 8.5 than RCP 4.5 and the slopes are higher for winter months compared to summer months.

Table 2

The slope of trends in annual sum of precipitation [mm *per* year] simulated by four climate models. LCI and UCI denote lower and upper confidence intervals at the 0.05 significance level, respectively.

Model	RCP 4.5			RCP 8.5		
	LCI	Slope	UCI	LCI	Slope	UCI
CanESM2	1.60	2.23	2.88	4.00	4.76	5.50
NorESM1-M	1.53	2.05	2.54	2.28	2.78	3.31
EC-Earth	1.77	2.29	2.82	3.70	4.26	4.86
MPI-ESM-LR	0.77	1.42	2.06	1.45	2.11	2.76
Ensemble median	1.57	2.14	2.68	2.99	3.52	4.08

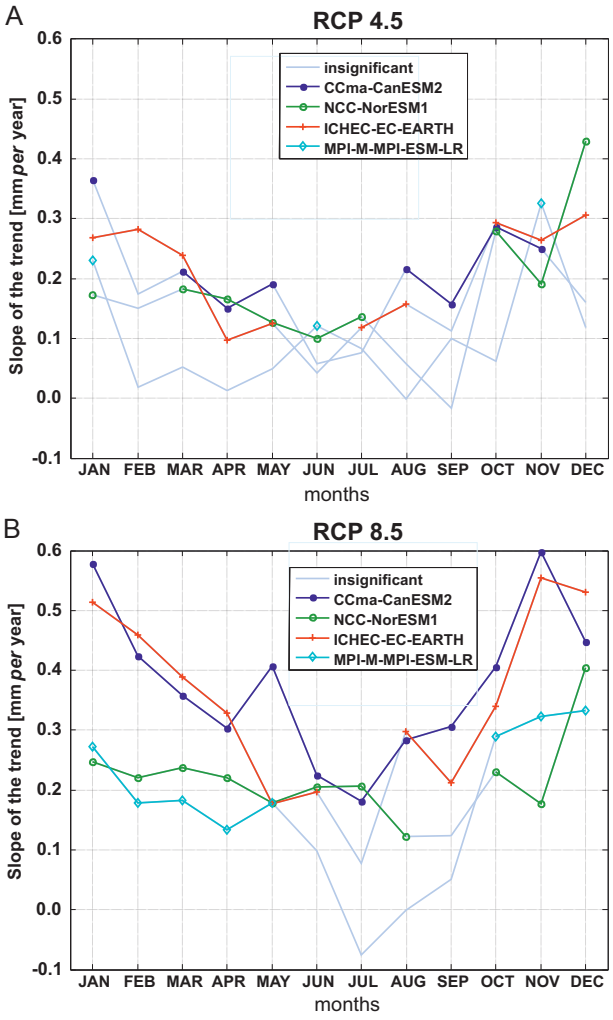

Fig. 8. Slope of trend [mm *per* year] estimated for monthly sum of precipitation over the period 1976–2100 using four climate models and two emission scenarios: RCP 4.5 (**A**) and RCP 8.5 (**B**). The light grey colour denotes lack of a statistically significant trend at the 0.05 significance level.

Climatic projections 2006–2100. Changes in air temperature. — The estimated values of mean annual air temperature in the three periods using four climate models are shown in Table 3. The results indicate positive changes with time for all models and for all emission scenarios. There are significant differences in the estimated values and also in tendencies of changes between climate models. The estimated changes between the near future (2021–2050) and reference period (1976–2005) for scenario RCP 4.5 vary from 2.7°C to 5.8°C. In the case of scenario RCP 8.5, these differences are higher, varying from 3.6 to 6.8°C.

Table 3

Comparison of mean annual air temperature [°C] in the three periods: ref (1976–2005), clim1 (2021–2050) and clim2 (2071–2100) following different emission scenarios.

	CanESM2	NorESM1-M	EC-Earth	MPI-ESM-LR
1976–2005	-3.4	-6.9	-8.7	-3.7
2021–2050 RCP 4.5	-0.1	-2.8	-2.9	-1.0
2021–2050 RCP 8.5	0.4	-2.5	-1.9	-0.1
2071–2100 RCP 4.5	1.9	-0.6	-0.4	0.5
2071–2100 RCP 8.5	4.8	1.2	3.7	3.4

The changes in mean annual air temperature between the far future and reference period are more severe. The climate models project an increase of air temperature from 4.2 to 8.3°C for scenario RCP 4.5 and from 7.1 to 12.4°C for RCP 8.5. All climate model simulations project the mean annual air temperature in the 2071–2100 period to be higher than 0°C following scenario RCP 8.5.

The analyses of air temperature changes on a monthly scale are presented in Fig. 9. The upper two charts present estimated results of changes for 2021–2050 with reference to the 1976–2005 period. The comparison indicates that projected changes are unevenly distributed throughout the year. The smallest changes and also the smallest variability between models were simulated for summer months. The projections for winter months (December–February) are characterized by higher increases of air temperature than for summer months. The median change from the ensemble of climate models is higher than 5°C. Additionally, the spread of results between the climate models, as shown by the error bars, indicate high uncertainties due to climate models for winter months.

Climatic projections 2006–2100. Changes in precipitation. — The estimated changes in mean annual sums of precipitation in the two future periods are presented in Table 4. The results vary between climate models but all models project an increase of precipitation totals for both periods and emission scenarios. Taking into account the relative changes between the near future and reference periods, the projected increases vary from 9% for MPI-ESM-LR following RCP 4.5 to 31% for EC-Earth following RCP 8.5. The results for the far future indicate higher increases of yearly sum of precipitation varying from 16% for MPI-ESM-LR following RCP 4.5 to 75% for EC-Earth following RCP 8.5. The comparison of results between emission scenarios (RCP 4.5 and RCP 8.5) indicates higher changes of precipitation for MPI-ESM-LR model following RCP 8.5 than following RCP 4.5. The other three model simulations show almost no difference in precipitation increases in the near future for emission scenarios RCP 4.5 and RCP 8.5.

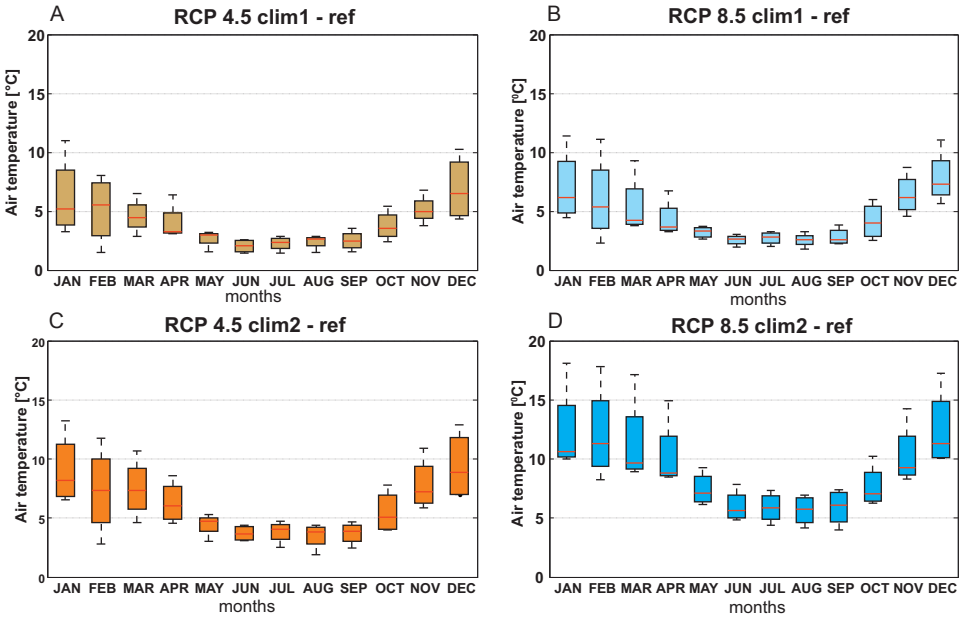

Fig. 9. Comparison of changes in air temperature between two future periods: clim1 (2021–2050; **A**, **B**) and clim2 (2071–2100; **C**, **D**) with reference period (1976–2005) for two emission scenarios, RCP 4.5 and RCP 8.5, using the results of four climate models. In each boxplot, the bottom and top of the box represent the first and third quartiles and the red line inside the box represents the median. The error bars represent the minimum and maximum from all climate models.

Table 4

Comparison of relative changes in mean annual sum of precipitation [%] in the two future periods: 2021–2050 and 2071–2100 with respect to 1976–2005 following different emission scenarios.

	CanESM2	NorESM1-M	EC-Earth	MPI-ESM-LR
2021–2050 RCP 4.5	22	24	29	9
2021–2050 RCP 8.5	21	24	31	18
2071–2100 RCP 4.5	30	38	36	16
2071–2100 RCP 8.5	56	42	75	24

The results of projected relative changes for monthly precipitation totals are shown in Fig. 10. Two panels in the upper row present results of changes between the near future and the reference period while the lower ones show the differences between the far future and the reference period. The panels located on the left show outcomes for emission scenario RCP 4.5, while those on the right give results for RCP 8.5 scenario. The estimated median relative

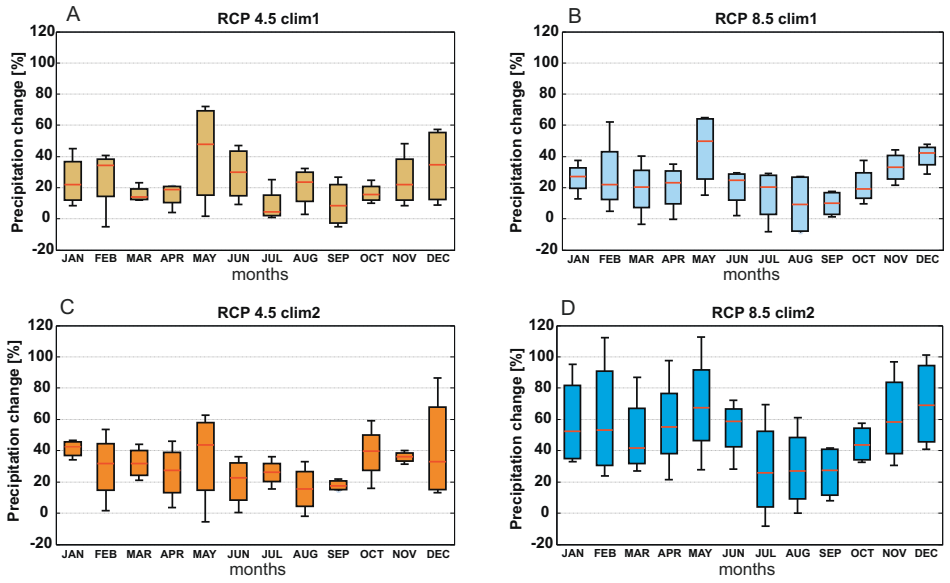

Fig. 10. Comparison of relative changes in monthly sum of precipitation between two future periods: clim1 (2021–2050; **A**, **B**) and clim2 (2071–2100; **C**, **D**) with reference period (1976–2005) for two emission scenarios RCP 4.5 and RCP 8.5 using the results of four climate models. In each boxplot, the bottom and top of the box represent the first and third quartiles, the red line inside the box represents the median, and the error bars represent the minimum and maximum of all of the data.

changes in precipitation from an ensemble of climate models for the near future (2021–2050) period for RCP 4.5 (upper row on the left) are positive in all cases and vary from 4% in July to 48% in May. The results from the four tested climate models differ in the estimated magnitudes and tendencies of changes. In a limited number of cases, one of the tested models indicates the opposite tendency of changes (February and September), however most of simulations project an increase in the monthly sum of precipitation. The spread in the estimated changes between climate models is shown in Fig. 10 by the error bars. For nine of months, the difference between the maximum and minimum estimated relative change of mean monthly precipitation is higher than 20%. In the other three months (March, April, and October), the spread of estimated relative changes between models is smaller than 20%. A comparison of the projections using the two emission scenarios for the near future indicates that the results for RCP 8.5 are characterized by higher changes in most of months except February, June, and August.

The projected changes of the mean monthly sum of precipitation between the reference period and the far future are presented in lower row of Figure 10.

The results indicate larger changes than those estimated for the near future. The median changes vary from 15% in August up to 44% in May for emission scenario RCP 4.5. In that case, the seasonal pattern of changes is most pronounced with smaller changes in the summer season and higher changes in the winter. Similar to the results for the near future, the outcomes from simulations following emission scenario RCP 8.5 give higher changes of mean monthly precipitation than RCP 4.5. The estimated median changes from an ensemble of climate models for RCP 8.5 vary from 26% in July to 69% in December. The results from different climate models are characterized by the high spread in the magnitude of changes (88% in February).

Classification of present and future climate of Southern Spitsbergen. — The largest changes in climatic conditions compared to the reference period were achieved for simulations of the far future (2071–2100) following emission scenario RCP 8.5. In that case, significant increases of air temperature and precipitation totals were estimated. These changes may result in changes of the characteristic features of Hornsund and Southern Spitsbergen climate. The simulated mean monthly air temperature over the 2071–2100 period (median from the ensemble of climate models) is slightly below 0°C in four months (December–March) with a minimum in March (-1.5°C). According to projections, the maximum mean monthly temperature (10.1°C) will be observed in July. As presented in Fig. 11, the results for monthly precipitation total indicate significant increases of late autumn-winter precipitation and small increases of precipitation in summer months.

The most widely used climate classification system is the one described by Köppen (1931). It is based upon annual and monthly means of temperature and precipitation, and uses natural vegetation boundaries as an expression of climate. Our estimates of air temperature and precipitation result in a different classification of Köppen climate type in Southern Spitsbergen than in the reference period. According to the criteria described in Gnanadesikan and Stouffer (2006), present climatic conditions in Southern Spitsbergen are classified as Polar tundra Et (area covered by tundra with $0°C < T_{max} < 10°C$ and $T_{min} < -3°C$). According to projections, the climatic conditions in the far future would be classified as a maritime subarctic climate or subpolar oceanic climate (Cfc). The subpolar oceanic climate characterises areas located close to the Polar region including parts of coastal Iceland, the Faroe Islands and coastal areas of north-western Norway (Tromsø region). If Southern Spitsbergen climate were to make this projected shift to a subpolar oceanic climate, milder winters and snowfall would tend to be more common. A subpolar oceanic climate features only one to three months of average monthly temperatures that are at least 10°C and none of its average monthly temperatures falls below -3°C. The potential impact of projected future air temperature and precipitation would influence vegetation cover and entire ecosystems.

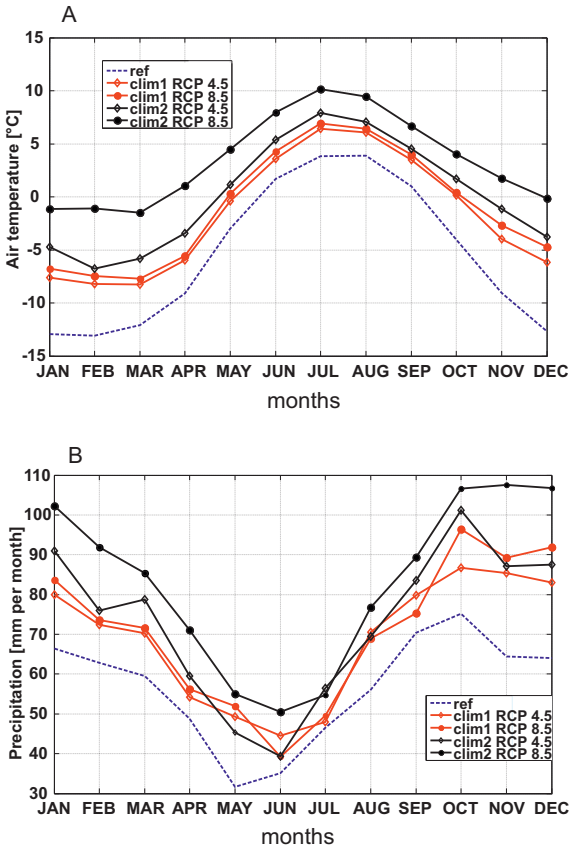

Fig. 11. A comparison of the simulated monthly median air temperature (**A**) and monthly total precipitation (**B**) over the reference period (1976–2005) and two future periods clim1 (2021–2050) and clim2 (2071–2100) for two emission scenarios RCP 4.5 and RCP 8.5.

Conclusions

In this study, the climate projections of air temperature and precipitation for the Southern Spitsbergen area were derived. The climatic variables were obtained from the Polar-CORDEX initiative in the form of a time series of daily air temperature and precipitation derived from four GCMs following RCP 4.5 and RCP 8.5 emission scenarios for the time period 1976–2100. The quality of these simulations were analysed by the comparison of simulations and observations at the Polish Polar Station *Hornsund* in the 1979–2005 period. Two climate models underestimated the observed air temperature and the two other models resembled observations. In the case of precipitation, all models overestimated the observed monthly sum of precipitation throughout the year except for during summer months.

Next, the changes of air temperature and precipitation over two future periods were estimated with reference to the period 1976–2005. The projections of air temperature were consistent; all analysed climate models simulated an increase of air temperature with time. Analyses of changes on a monthly scale indicated that the highest increases were estimated for winter months. For emission scenario RCP 8.5 in the far future (2071–2100), winter temperatures were simulated to be up to 11°C higher than in the reference period.

The analyses of monthly and annual sum of precipitation also indicated increasing tendencies of change with time, although results for some months and climate models differ in the direction of changes. The differences between mean monthly sum of precipitation for the near future (2021–2050) and the reference period (1976–2005) were similar between months. In the case of changes between far future and reference period, the highest increases were projected for the winter months.

The projections for 2071–2100 period following RCP 8.5 scenario indicate that annual course of air temperature in Southern Spitsbergen will resemble present climatic conditions of subarctic maritime climate, with winter temperatures slightly below 0°C, longer summer seasons than recently observed, maximum precipitation in autumn and early winters, and relatively dry summers. This climatic shift may result in the prolongation of the ablation season with associated impacts on the hydrological system. A combination of changes in air temperature and precipitation may lead to changes that would have significant influence on ground thermal conditions, water balance and glacier extensions. Additionally, critical variables such as soil moisture, groundwater recharge and runoff that control all ecosystems may be affected.

Acknowledgements. — The study was supported from the project Climate Change Impacts on Hydrological Extremes (CHIHE) Pol-Nor/196243/80/2013, which is supported by the Norway-Poland Grants Program administered by the Norwegian Research Council and by the Polish National Science Centre through grant no. 2013/09/N/ST10/04105: *Impact of climate change on snow cover and hydrological regime of polar non-glaciated catchment*. We are grateful to the reviewers Jūratė Kriaučiūnienė and Joanna Wibig for valuable comments on the manuscript. The final stage was supported by the Centre for Polar Studies KNOW Leading National Research Centre, Poland, and statutory activities of the Polish Ministry of Science and Higher Education (3841/E-41/S/2016).

References

ACIA 2005. *Arctic Climate Impact Assessment*, Cambridge University Press: 1042 pp.

BEDNORZ E. and KOLENDOWICZ L. 2013. Summer mean daily air temperature extremes in Central Spitsbergen. *Theoretical and Applied Climatology* 113: 471–479.

BINTANJA R. and VAN DER LINDEN E.C. 2013. The changing seasonal climate in the Arctic. *Scientific Reports* 3: 1556.

CHRISTENSEN J.H., BOBERG F., CHRISTENSEN O.B. and LUCAS-PICHER P. 2008. On the need for bias correction of regional climate change projections of temperature and precipitation. *Geophysical Research Letters* 35: L20709.

COHEN J., SCREEN J.A., FURTADO J.C., BARLOW M., WHITTLESTON D., COUMOU D., FRANCIS J., DETHLOFF K., ENTEKHABI D., OVERLAND J. and JONES J. 2014. Recent Arctic amplification and extreme mid-latitude weather. *Nature Geoscience* 7: 627–637.

EHRET U., ZEHE E., WULFMEYER V., WARRACH-SAGI K. and LIEBERT J. 2012. Should we apply bias correction to global and regional climate model data? *Hydrology and Earth System Sciences* 16: 3391–3404.

FØRLAND E.J., BENESTAD R., HANSSEN-BAUER I., HAUGEN J.E. and SKAUGEN T.E. 2011. Temperature and precipitation development at Svalbard 1900–2100. *Advances in Meteorology*, 893790.

GIORGI F., JONES C. and ASRAR G.R. 2009. Addressing climate information needs at the regional level: the CORDEX framework. *WMO Bulletin* 58: 175–183.

GLISAN J.M. and GUTOWSKI W.J. JR. 2014. WRF summer extreme daily precipitation over the CORDEX Arctic. *Journal of Geophysical Research: Atmospheres* 119: 1720–1732.

GLISAN J.M., GUTOWSKI W.J. JR., CASSANO J.J. and HIGGINS M.E. 2013. Effects of spectral nudging in WRF on Arctic temperature and precipitation simulations. *Journal of Climate* 26: 3985–3999.

GNANADESIKAN A. and STOUFFER R.J. 2006. Diagnosing atmosphere-ocean general circulation model errors relevant to the terrestrial biosphere using the Köppen climate classification. *Geophysical Research Letters* 33: DOI: 10.1029/2006GL028098.

GOOSSE H. 2015. *Climate System Dynamics and Modelling*. Cambridge University Press: 273 pp.

HAMED K.H. and RAO R. 1998. A modified Mann-Kendall trend test for autocorrelated data. *Journal of Hydrology* 204: 182–196.

KATTSOV V.M. and WALSH J.E. 2000. Twentieth-century trends of Arctic precipitation from observational data and a climate model simulation. *Journal of Climate* 13: 1362–1369.

KENDALL M.G. 1975. *Rank Correlation Methods*. Charles Griffin, London: 260 pp.

KOENIGK T., BERG P. and DOSCHER R. 2015. Arctic climate change in an ensemble of regional CORDEX simulations. *Polar Research* 34: 24603.

KÖPPEN W. 1931. *Grundriss der Klimakunde*. Walter de Gruyter, Berlin: 388 pp.

KUNDZEWICZ Z. and ROBSON A. 2004. Change detection in hydrological records — a review of the methodology. *Hydrological Sciences Journal* 49: 7–19.

LARSEN J.N., ANISIMOV O.A., CONSTABLE A., HOLLOWED A.B., MAYNARD N., PRESTRUD P., PROWSE T.D. and STONE J.M.R. 2014. Polar regions. *In*: V.R. Barros, C.B. Field, D.J. Dokken, M.D. Mastrandrea, K.J. Mach, T.E. Bilir, M. Chatterjee, K.L. Ebi, Y.O. Estrada, R.C. Genova, B. Girma, E.S. Kissel, A.N. Levy, S. MacCracken, P.R. Mastrandrea and L.L. White (eds) *Climate Change 2014: Impacts, Adaptation, and Vulnerability. Part B: Regional Aspects. Contribution of Working Group II to the Fifth Assessment Report of the Intergovernmental Panel on Climate Change*. Cambridge University Press, Cambridge, United Kingdom and New York, NY, USA: 1567–1612.

MADSEN H., LAWRENCE D., LANG M., MARTINKOVA M. and KJELDSEN T.R. 2014. Review of trend analysis and climate change projections of extreme precipitation and floods in Europe. *Journal of Hydrology* 519: 3634–3650.

MANN H. 1945. Nonparametric tests against trend. *Econometrica* 13: 245–259.

MATTHES H., RINKE A., MILLER P., KUHRY P. and DETHLOFF K. 2011. Sensitivity of high-resolution Arctic regional climate model projections to different implementations of land surface processes. *Climatic Change* 111: 197–214.

MILLER G.H., ALLEY R.B., BRIGHAM-GRETTE J., FITZPATRICK J.J., POLYAK L., SERREZE M.C. and WHITE J.W.C. 2010. Arctic amplification: can the past constrain the future? *Quaternary Science Reviews* 29: 1779–1790.

MOSS R.H., EDMONDS J.A., HIBBARD K.A., MANNING M.R., ROSE S.K., VAN VUUREN D.P., CARTER T.R., EMORI S., KAINUME M., KRAM T., MEEHL G.A., MITCHELL J.F.B., NAKICENOVIC N., RIAHI K., SMITH S.J., STOUFFER R.J., THOMSON A.M., WEYANT J.P. and WILBANKS T.J. 2010. The next generation of scenarios for climate change research and assessment. *Nature* 463: 747–756.

MUERTH M.J., GAUVIN ST-DENIS B., RICARD S., VELÁZQUEZ J.A., SCHMID J., MINVILLE M., CAYA D., CHAUMONT D., LUDWIG R. and TURCOTTE R. 2013. On the need for bias correction in regional climate scenarios to assess climate change impacts on river runoff. *Hydrology and Earth System Sciences* 17: 1189–1204.

NAKICENOVIC N., ALCAMO J., DAVIS G., FENHANN J., GAFFIN S., GREGORY K., GRÜBLER A., JUNG T.Y., KRAM T., LA ROVERE E.L., MICHAELIS L., MORI S., MORITA T., PEPPER W., PITSCHER H., PRICE L., RAIHI K., ROEHRL A., ROGNER H.-H., SANKOVSKI A., SCHLESINGER M., SHUKLA P., SMITH S., SWART R., CAN ROOIJEN S., VICTOR N., DE VRIES B. and DADI Z. 2000. *Emissions Scenarios. A Special Report of Working Group III of the Intergovernmental Panel on Climate Change*. Cambridge University Press, Cambridge, United Kingdom and New York, NY, USA: 599 pp.

NORDLI Ø., PRZYBYLAK R., OGILVIE A.E.J. and ISAKSEN K. 2014. Long–term temperature trends and variability on Spitsbergen: the extended Svalbard Airport temperature series 1898–2012. *Polar Research* 33: 21349.

OSUCH M., ROMANOWICZ R.J., LAWRENCE D. and WONG W.K. 2016. Trends in projections of standardized precipitation indices in a future climate in Poland. *Hydrology and Earth System Sciences* 20: 1947–1969.

OVERLAND J.E., WOOD K.R. and WANG M. 2011. Warm Arctic—cold continents: climate impacts of the newly open Arctic Sea. *Polar Research* 30: 15787.

OVERLAND J.E., WANG M., WALSH J.E. and STROEVE J.C. 2014. Future Arctic climate changes: adaptation and mitigation timescales. *Earth's Future* 2: 68–74.

PRZYBYLAK R. 2003. Scenarios of the Arctic Future Climate. *In*: R. Przybylak (Ed) *The Climate of the Arctic*, Volume 52 of series Atmospheric and Oceanographic Sciences Library: 245–279.

PRZYBYLAK R., ARAŹNY A., NORDLI Ø., FINKELNBURG R., KEJNA M., BUDZIK T., MIGAŁA K., SIKORA S., PUCZKO D., RYMER K. and RACHLEWICZ G. 2014. Spatial distribution of air temperature measurements on Svalbard during 1 year with campaign measurements. *International Journal of Climatology* 34: 3702–3719.

RINKE A. and DETHLOFF K. 2008. Simulated circum-Arctic climate changes by the end of the 21st century. *Global and Planetary Change* 62: 173–186.

RINKE A., DETHLOFF K., CASSANO J.J., CHRISTENSEN J.H., CURRY J.A., DU P., GIRARD E., HAUGEN J.-E., JACOB D., JONES C.G., KØLTZOW M., LAPRISE R., LYNCH A.H., PFEIFER S., SERREZE M.C., SHAW M.J., TJERNSTRÖM M., WYSER K. and ZAGAR M. 2006. Evaluation of an ensemble of Arctic regional climate models: Spatiotemporal fields during the SHEBA year. *Climate Dynamics* 26: 459–472.

RINKE A., MATTHES H., CHRISTENSEN J.H., KUHRY P., ROMANOVSKY V. and DETHLOFF K. 2011. Arctic RCM simulations of temperature and precipitation derived indices relevant to future frozen ground conditions. *Global and Planetary Change* 80–81: 136–148.

SERREZE M.C., BARRETT A.P., STROEVE J.C., KINDIG D.N. and HOLLAND M.M. 2009. The emergence of surface-based Arctic amplification. *Cryosphere* 3: 11–19.

SOLOMON S., QIN D., MANNING M., CHEN Z., MARQUIS M., AVERYT K.B., TIGNOR M. and MILLER H.L. 2007. *Climate change 2007: Contribution of Working Group I to the Fourth Assessment Report of the Intergovernmental Panel on Climate Change*. Cambridge University Press, Cambridge, United Kingdom and New York, NY, USA: 996 pp.

STOCKER T.F., QIN D., PLATTNER G.-K., TIGNOR M., ALLEN S.K., BOSCHUNG J., NAUELS A., XIA Y., BEX V. and MIDGLEY P.M. 2013. *Climate Change 2013: The Physical Science Basis. Contribution of Working Group I to the Fifth Assessment Report of the Intergovernmental Panel on Climate Change*. Cambridge University Press, Cambridge, United Kingdom and New York, NY, USA: 1535 pp.

SUNYER M.A., HUNDECHA Y., LAWRENCE D., MADSEN H., WILLEMS P., MARTINKOVA M., VORMOOR K., BÜRGER G., HANEL M., KRIAUČIŪNIENĖ J., LOUKAS A., OSUCH M. and YÜCEL I. 2015. Inter-comparison of statistical downscaling methods for projection of extreme precipitation in Europe. *Hydrology and Earth System Sciences* 19: 1827–1847.

TEUTSCHBEIN C. and SEIBERT J. 2013. Is bias correction of regional climate model (RCM) simulations possible for nonstationary conditions? *Hydrology and Earth System Sciences* 17: 5061–5077.

VORMOOR K., LAWERNCE D., HEISTEMANN M. and BRONSTERT A. 2015. Climate change impacts on the seasonality and generation processes of floods – projections and uncertainties for catchments with mixed snowmelt/rainfall regimes. *Hydrology and Earth System Sciences* 19: 913–931.

WAWRZYNIAK T., OSUCH M., NAPIÓRKOWSKI J.J. and WESTERMANN S. 2016. Modelling of the thermal regime of permafrost during 1990–2014 in Hornsund, Svalbard. *Polish Polar Research* 37: 219–242.

WILCOX R.R. 2005. Theil–Sen estimator. *In*: R.R. Wilcox (Ed), *Introduction to Robust Estimation and Hypothesis Testing*. Academic Press, San Diego: 423–427.

WIBIG J., JACZEWSKI A., BRZÓSKA B., KONCA-KĘDZIERSKA K. and PIANKO-KLUCZYŃSKA K. 2014. How does the areal averaging influence the extremes? The content of gridded observation data sets. *Meteorologisch Zeitschrift* 23: 181–187.

Received 16 December 2015
Accepted 7 April 2016